Versatile Glycoblotting Nanoparticles for High-Throughput Protein Glycomics

Kenichi Niikura,[a] Ryosuke Kamitani,[a] Masaki Kurogochi,[a] Rie Uematsu,[a] Yasuro Shinohara,[a] Hiroaki Nakagawa,[a] Kisaburo Deguchi,[a] Kenji Monde,[a] Hirosato Kondo,[b] and Shin-Ichiro Nishimura*[a, c]

Abstract: We have developed an effective and practical trap-and-release method based on chemoselective ligation of carbohydrates with reactive aminooxyl groups attached to the surface of nanoparticles (referred to as glycoblotting nanoparticles). These glycoblotting nanoparticles were synthesized by UV irradiation of diacetylene-functionalized lipids that contain the aminooxyl group. The glycoblotting nanoparticles captured carbohydrates in aqueous solution under mild conditions and were collected by simple centrifugation. The trapped carbohydrates were effectively released from the nanoparticles under acidic conditions to give pure oligosaccharides. This glycoblotting process reduced the time required for the purification process of carbohydrates to less than 6 h, compared to the several days needed for conventional chromatographic techniques. The oligosaccharides (*N*-glycan) were released from ovalbumin (glycoprotein) by PNGase F after tryptic digestion. MALDI-TOF mass spectra before purification did not show any significant signals corresponding to *N*-glycans because these signals were hidden by the large signals of the abundant peptides. However, after purification with the glycoblotting nanoparticles, only signals corresponding to oligosaccharides appeared. We also demonstrated a clear analysis of the oligosaccharides contained in the mice dermis by means of glycoblotting.

Keywords: glycoblotting · glycosylation · high-throughput screening · mass spectrometry · nanoparticles

Introduction

Many proteins are posttranslationally modified by glycosylation, and in numerous cases, these glycosylated entities are specifically responsible for their function. Recent data indicate that more than half of all human proteins are glycosylated.[1] Changes in the extent of glycosylation and the structure of carbohydrates on the cell surface and proteins have been proved to correlate with cancer and other diseases. For example, the *N*-glycans in the IgG from patients with rheumatoid arthritis are deficient in galactose and contained increased levels of two-terminal *N*-acetylglucosamine glycoforms.[2] It is also known that unique carbohydrates attach to tumor cells and work as tumor markers for cancers such as pancreatic and colon cancer.[3] Therefore, it is expected that a method for the systematic and quantitative analysis of glycoproteins would be very useful for the screening of new potential biomarkers for diagnosis and therapeutic targets.

To decipher and screen the information contained in complex carbohydrates, general and readily accessible techniques for high-throughput analysis of molecular glycosylation must be developed. In many cases, the target carbohydrates are contained in crude biological samples. Conventional chromatographic techniques have faced difficulties with the purification process of trace amounts of oligosaccharides in a crude mixture containing an abundance of digested residues of proteins and impurities. Affinity columns based on lectins (naturally occurring protein receptors for carbohydrate structures) have often been used to isolate specific car-

[a] Dr. K. Niikura, R. Kamitani, Dr. M. Kurogochi, R. Uematsu, Dr. Y. Shinohara, Dr. H. Nakagawa, Dr. K. Deguchi, Dr. K. Monde, Prof. S.-I. Nishimura
Division of Biological Sciences, Graduate School of Science
Frontier Research Center for Post-Genome Science and Technology, Hokkaido University
Kita 21 Nishi 8, Kita-ku, Sapporo 001–0021 (Japan)
E-mail: shin@glyco.sci.hokudai.ac.jp

[b] Dr. H. Kondo
Discovery Research Laboratories, Shionogi & Co., Ltd., Osaka 553–0002 (Japan)

[c] Prof. S.-I. Nishimura
National Institute of Advanced Industrial Science and Technology (AIST), Sapporo 062–8517 (Japan)

 DOI: 10.1002/chem.200401289

bohydrates.[4] However, their high specificity makes any single lectin ineffective for capturing all glycoforms existing on glycoproteins. Reinold reported a sugar-trapping method in which carbohydrates that were activated with hydrazine can be trapped by an aldehydic polymer.[5] We recently reported a technique that used oxylamine-functionalized glycoblotting polymers for rapid glycoform analysis of glycoproteins.[6] After releasing the carbohydrates from the glycoproteins, all released structures in oligosaccharides have an identical exposed hemiacetal-reducing terminus that provides a single reactive moiety for covalent capture. Released oligossacharides can be directly trapped by hemiacetal-reactive groups, such as oxylamine and hydrazide. Fischer found that the reaction of oligosaccharides with phenylhydrazine proceeds smoothly to give the corresponding stable phenylhydrazone derivatives under mild conditions.[7] Mutter reported that aminooxyl groups are also reactive with the hemiacetal of the carbohydrate through a stable oxime bond.[8] Herein, we present an effective and practical trap-and-release method based on chemoselective ligation of carbohydrates with oxylamino groups attached to the surface of nanoparticles (Figure 1) and describe the optimal conditions for glycoblotting and the versatility of this method. We have chosen an oxylamine-functionalized photopolymerizable lipid as an anchor molecule for capturing oligosaccharides. Liposomes of diacetylene-containing lipids can be readily polymerized by UV irradiation to produce stable polymer-based nanoparticles,[9,10] The nanoparticles were simply collected by centrifugation after trapping the carbohydrates, which were then released from the particles under acidic conditions. Our approach significantly shortens the sugar-purification process. Our method was applied to the analysis of the glycosylation pattern of serum glycoproteins and mice dermis.

Results and Discussion

Syntheses of photopolymerizable lipids and glycoblotting: Previously, we reported an optical sensing technique for sugar–protein interactions by means of sugar-functionalized polydiacetylene-based nanoparticles.[11] The polydiacetylene nanoparticles can readily be prepared from photopolymerizable liposomes. The nanoparticles are stable and well-dispersed in aqueous solution. The good solubility in aqueous solutions and a large surface area resulting from their size contribute to making the nanoparticles an effective trap for oligosaccharides in biological samples. Here, we used polydiacetylene-based nanoparticles as a scaffold to trap oligosaccharides. Photopolymerizable oxylamino-lipid **1** was syn-

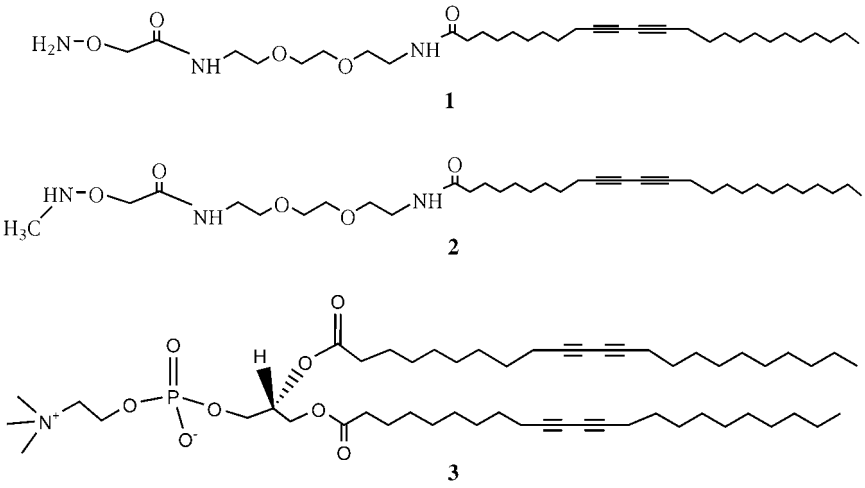

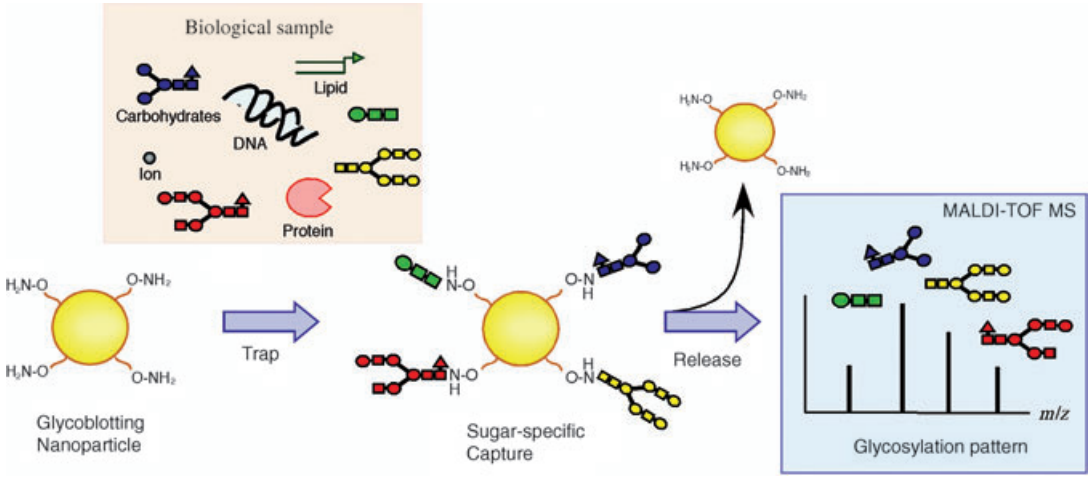

Figure 1. The concept of the trap-and-release based approach to glycopattern analysis using oxylamine-functionalized glycoblotting nanoparticles.

thesized according to Scheme 1. 2-[2-(2-Aminoethoxy)-ethoxy]ethylamine was attached to commercially available photopolymerizable 10,12-pentacosadyinoic acid (**4**) to generate **5** in the presence of water-soluble carbodiimide in 75% yield. Boc-protected oxylamino derivative **6** was introduced to the lipid **5** and the Boc group was removed under acidic conditions to generate target lipid **1**. *N*-methyl-aminooxyl lipid **2** was synthesized in a similar manner (Scheme 2). We used these lipid molecules to create aminooxyl-functionalized nanoparticles. The liposome was synthesized by a 3:7 molecular ratio mixture of aminooxyl lipid (**1** or **2**) and diacetylene phospholipid **3**. The polydiacetylene polymer was formed by 1,4-addition of the diacetylenic monomers, initiated by UV irradiation. The photopolymerization process was readily confirmed by UV/Vis spectroscopy (Figure 2a). The mean diameter of the nanoparticles was between 200–300 nm, as determined by scanning electronic microscopy (SEM) (Figure 2b). This size of nanoparticles is easily separable by centrifugation from sample biomolecules, such as peptide and proteins ($\approx$10 nm). The SEM image also demonstrates that the polymerized nanoparticles were stable under the vacuum conditions required for SEM measurements, whereas liposomes can not be visualized by SEM.

Trapping efficiency of glycoblotting nanoparticles: The carbohydrate-trapping capability of the glycoblotting nanoparticles was examined by means of surface plasmon resonance (SPR). The nanoparticles were immobilized on a BIAcore sensor chip and the binding of carbohydrates was monitored. A solution of the synthetic nanoparticles was deposit-

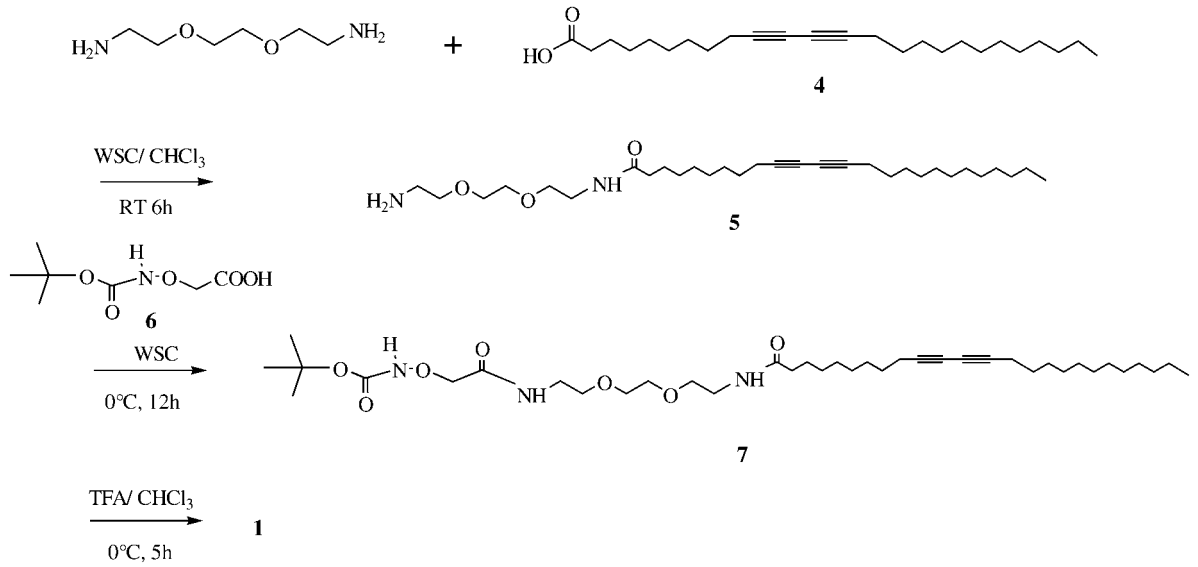

Scheme 1. Synthetic route to photopolymerizable hydroxylamino lipid **1**.

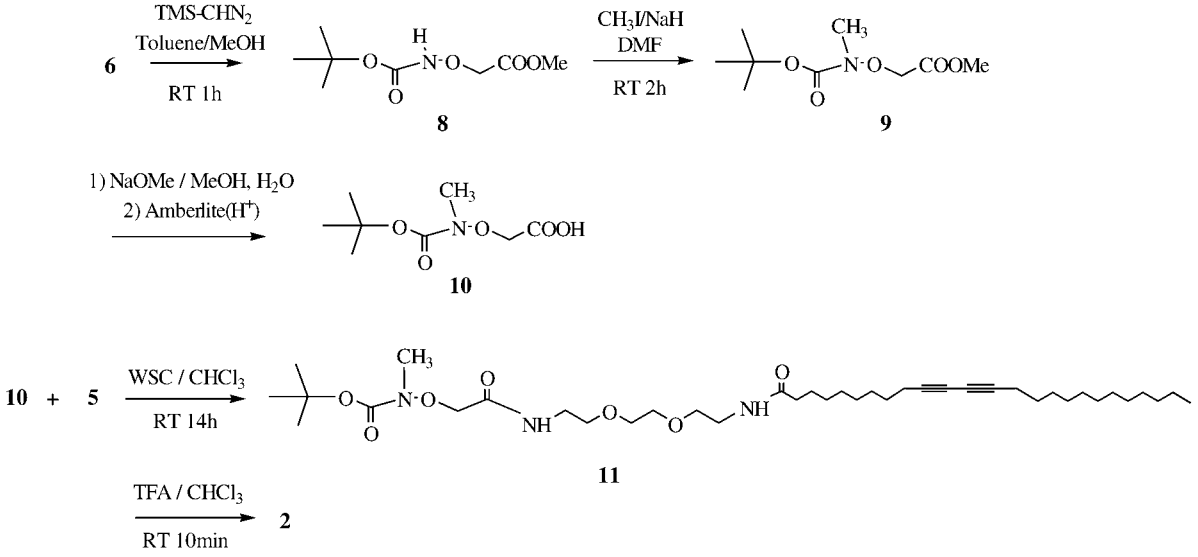

Scheme 2. Synthetic route to photopolymerizable *N*-methylaminooxyl lipid **2**.

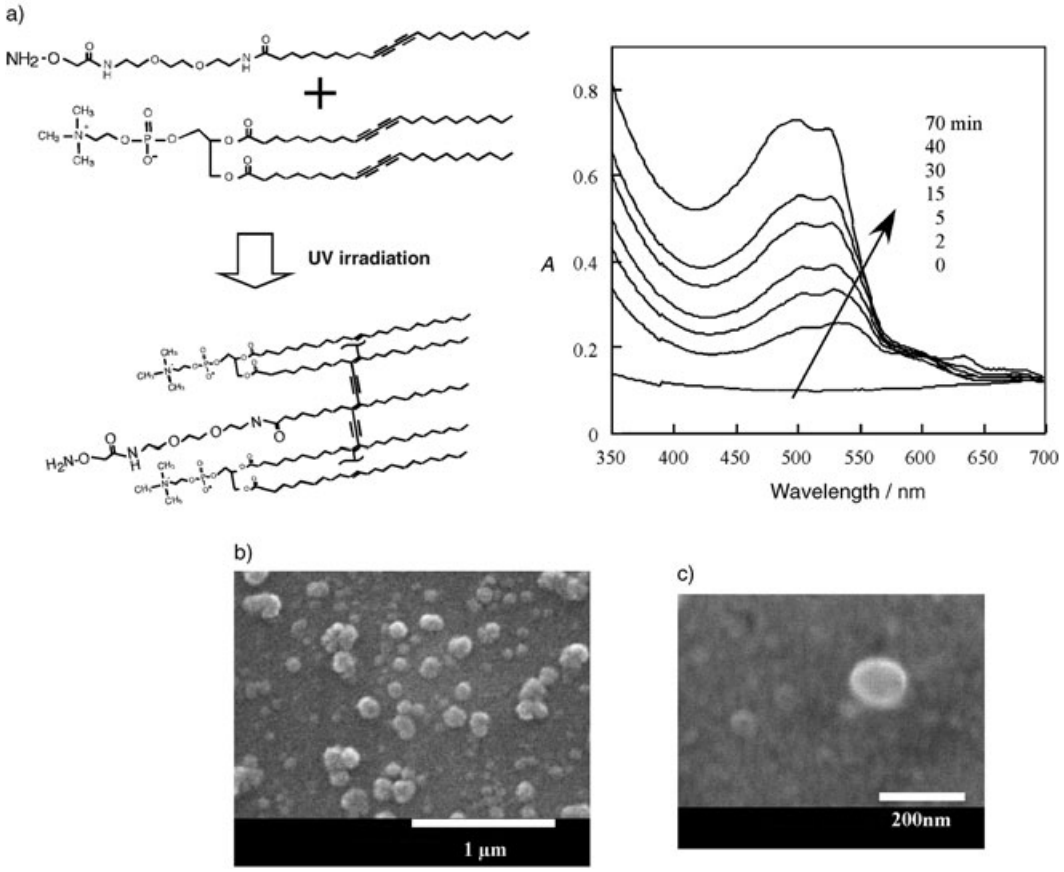

Figure 2. Photopolymerization of diacetylene-containing liposomes. a) Change in UV/Vis absorption spectra of the liposome **1/3** (3/7 mol/mol). The spectra were recorded after exposure to $\lambda = 254$ nm light for the indicated period. Scanning electron micrograph (SEM) of polymerized liposomes **1/3** from b) water and c) ethanol.

ed onto the C18-covered hydrophobic chip at pH 7.4, and the nanoparticles were immobilized by hydrophobic interaction.[12] A solution of mannopentaose (5 mg mL^{-1}) was then deposited onto the chip and an increase in signal intensity (ΔRU = 87) was observed (Figure 3). When cyclodextrin, which does not have the reducing end, is used instead of mannopentaose, there is no change in the signal intensity. This proves that the reducing end of the carbohydrates is the reactive moiety for binding to the nanoparticles. The reaction efficiency between nanoparticles and carbohydrates was quantitatively estimated by means of a conventional sulfuric acid/methylresorcinol method, which is based on the measurement of the optical absorption at $\lambda = 425$ nm.[13] The trapping efficiency of the synthetic nanoparticles (lipids **1** and **3** = 3:7 mol mol^{-1}) was evaluated with *N*-acetyllactosamine (LacNAc) in an acetate buffer (10 mM, pH 4.2). LacNAc was used as a model carbohydrate for *N*-glycans because *N*-glycans commonly contains GlcNAc at the reducing end. The nanoparticles were incubated with LacNAc (0.1 mg, 26 μmol) at 40 °C for 3 h. The

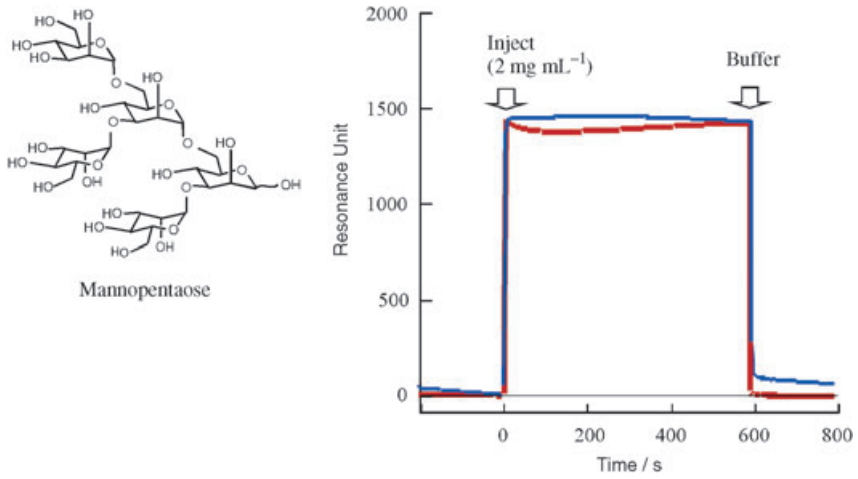

Figure 3. The binding behaviors of mannnopentaose (blue) and CD (red) with respect to the glycoblotting nanoparticle immobilized on a surface plasmon resonance (SPR) sensor chip.

nanoparticles were easily removed from the solution by spin filtration. The yield of LacNAc trapped on the nanoparticles (lipid **1** and **3** = 3:7 mol mol^{-1}) was calculated by determining the free (unbound) LacNAc concentration in the filtrate by means of a sulfuric acid/methylresorcinol-based method. The yields of trapped LacNAc were plotted against the total aminooxyl residues on the nanoparticles (Figure 4). More

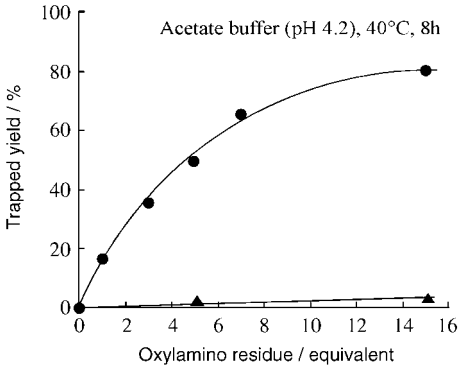

Figure 4. Plot of the trapping efficiency of *N*-acetyllactosamine (26 μmol as 1 equiv) with nanoparticles **1/3** (●) and **3** (▲) as a function of the aminooxyl residue equivalent in acetate buffer (pH 4.2), 40 °C.

than 80 % of the added LacNAc was trapped in the presence of a large excess of oxylaminoic nanoparticles. In a control experiment, nanoparticles without the aminooxyl groups on their surfaces showed no trapping of carbohydrates, indicating that the aminooxyl group on the glycoblotting nanoparticles is the functional moiety for the specific capturing of carbohydrates. When the nanoparticles with the aminooxyl group were incubated with cyclodextrins, no trapping of cyclodextrins by the nanoparticles was observed. We also investigated the effect of pH on the sugar-trapping efficiency with LacNAc (0.1 mg, 26 μmol). The nanoparticles (with a 5:1 excess of aminooxyl residues to LacNAc) captured the carbohydrate in a wide range of pH values, from 2 to 8, with a 50–70 % yield (data not shown). The maximum efficiency was observed at pH 4.2, which corresponds to the conditions in our previous report on the reaction between sugar and the oxylamino group.[6]

We prepared four kinds of glycoblotting particles (from **1**, **2**, **1/3** and **2/3**) and compared their trapping and recovery yields for LacNAc in acetate buffer (pH 4.2) at 37 °C (Figure 5). The trapping efficiency for LacNAc was ≈45 % for the nanoparticles constructed from lipid **1** or **2** alone. The release of carbohydrates from the nanoparticles was preformed by adding a TFA solution (total of 5 %). The total yields for both trapping and release process were almost identical with the trapping efficiencies, which showed that the efficiency is governed by the trapping process, and that the release process is almost quantitative under acidic conditions. The methylated oxylamino group reacts with carbohydrates through a cyclic oxime bond,[14] whereas the oxylamino group binds carbohydrates with a linear oxime bond. However, there is no significant difference in the trapping

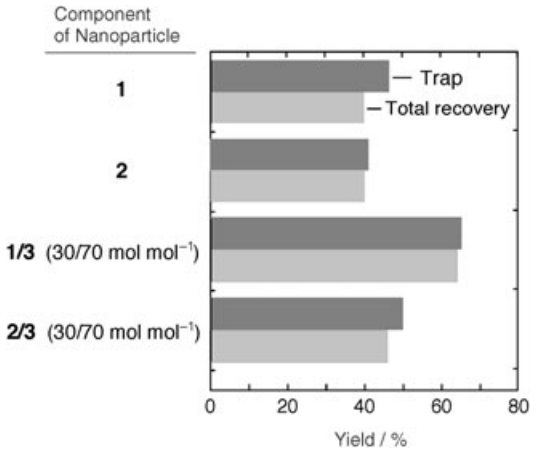

Figure 5. Trapped and recovered yield of *N*-acetyllactosamine from the glycoblotting nanoparticles (**1**, **2**, **1/3**, and **2/3**) in acetate buffer (pH 4.2) at 40 °C. Upper bar: trapped yield; bottom bar: recovered yield. Release of LacNAc from the nanoparticles was performed by adding TFA.

efficiency between the two nanoparticles synthesized from **1** or **2** alone. We used a phosphorylcholine-type lipid **3** as an important component to reduce the nonspecific attachment[15] of peptides contained in a sample to the surface of the nanoparticles. Addition of phosphorylcholine-type lipid **1** or **2** to the components of the nanoparticles led to an increase of the trapping yield. Since the **1/3** nanoparticles had the highest efficiency, all the following experiments were performed with that nanoparticle.

The release process was also confirmed by matrix-assisted laser desorption/ionization time-of-flight (MALDI-TOF) mass spectrometry. After glycoblotting of the carbohydrate (mannopentaose), the nanoparticles were cast on the MALDI-TOF plate with matrix molecules (2,5-dihydroxybenzoic acid). The bound carbohydrates were released from the nanoparticles by adding 5 % TFA aqueous solution. Figure 6 shows the MALDI-TOF spectra before and after TFA treatment. Before TFA treatment, the carbohydrate signal was very weak. After hydrolysis of the oxime bond

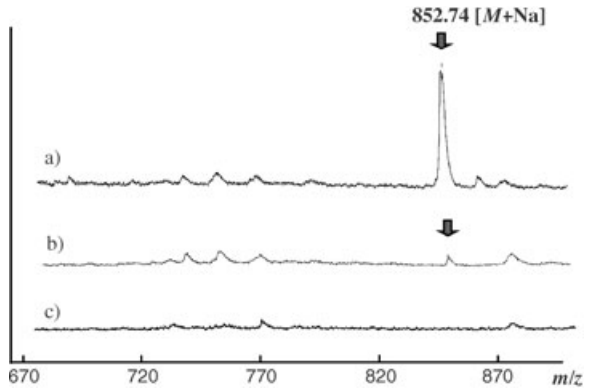

Figure 6. MALDI-TOF mass spectrum of mannopentaose released from the mannopentaose-containing nanoparticles (**1/3**). a) With TFA treatment, and b) without TFA treatment. c) TFA treatment was performed on the nanoparticle **3** after the trapping process (control).

with TFA, however, a clear signal appeared. As a control, the experiment was repeated with nanoparticles consisting only of lipid **3**, and no signal appeared after the TFA treatment.

Glycoblotting of *N*-glycans from glycoproteins and their MALDI-TOF mass analyses: We applied the glycoblotting approach to the analysis of oligosaccharides from a typical glycoprotein, ovalbumin. Ovalbumin (1 mg) was digested with protease (pronase and trypsin), and the subsequent deglycosylation of *N*-glycans from the glycopeptides was performed with PNGase F. We used the crude mixture (*N*-glycans in a large excess of peptides) as a model sample to examine the purification ability of the glycoblotting nanoparticles. The glycoblotting nanoparticles (5 mg mL^{-1}) were added to the crude solution (500 μL) and the pH was adjusted to 4.2. The solution was incubated for 5 h at 40 °C. The nanoparticles were then isolated by centrifugation with a Microcon YM-50. The nanoparticles were washed three times with pure water and then vortexed in water with an acidic resin functionalized with sulfonic acid (Amberlite 120) for 3 h at 37 °C to release the trapped carbohydrates. We used an acidic resin as the catalyst to release the carbohydrates because the acidic resin and the blotting nanoparticles can be removed from the oligosaccharide solution simultaneously. After the removal of the resin and the nanoparticles by centrifugation, the filtrate was analyzed by MALDI-TOF mass spectrometry in α-cyano-4-hydroxycinnaminic acid (CHCA) as the MALDI matrix. The total duration of the purification process requires ≈6 h. Only the signals corresponding to carbohydrates appeared after glycoblotting (Figure 7). The *N*-glycan structures of ovalbumin have already been reported[16] and the mass spectrometry data obtained correspond to those that were reported. Table 1 shows that all signals in Figure 7a accurately correspond to molecular weights of oligosaccharides containing hexose and *N*-acetylhexoamine. The crude mixture, on the other hand, gave numerous signals corresponding to impurities, such as degraded peptides, and no carbohydrate signals were observed owing to ion suppression by the peptides.

To prove that the signals in Figure 7a really do correspond to *N*-glycans and not to peptide contaminants, TOF/TOF analysis was carried out for each peak. We have previously reported that the fragmentation of the precursor ions by the LIFT-TOF/TOF method allows precise sequencing of *N*-glycans,[17, 18] A sample of a LIFT-TOF/TOF spectrum of *m*/*z* 1339.5 is shown in Figure 7b. The fragment ions clearly show a separation of 164 and 203, indicative of mass differences attributable to hexose (Hex) units and *N*-acetylhexosamine (HexNAc) units. For all signals, we confirmed that each signal provides fragmentation corresponding to Hex and HexNAc in the TOF/TOF spectra. LIFT fragmentation occurred predominantly at the glycoside bond between the two *N*-acetyl-D-glucosamine (GlcNAc) residues, whose fragments (lacking one GlcNAc) are shown with an asterisk. The following fragmentation occurred from the nonreducing end of the oligosaccharide, thus allowing sequencing of the

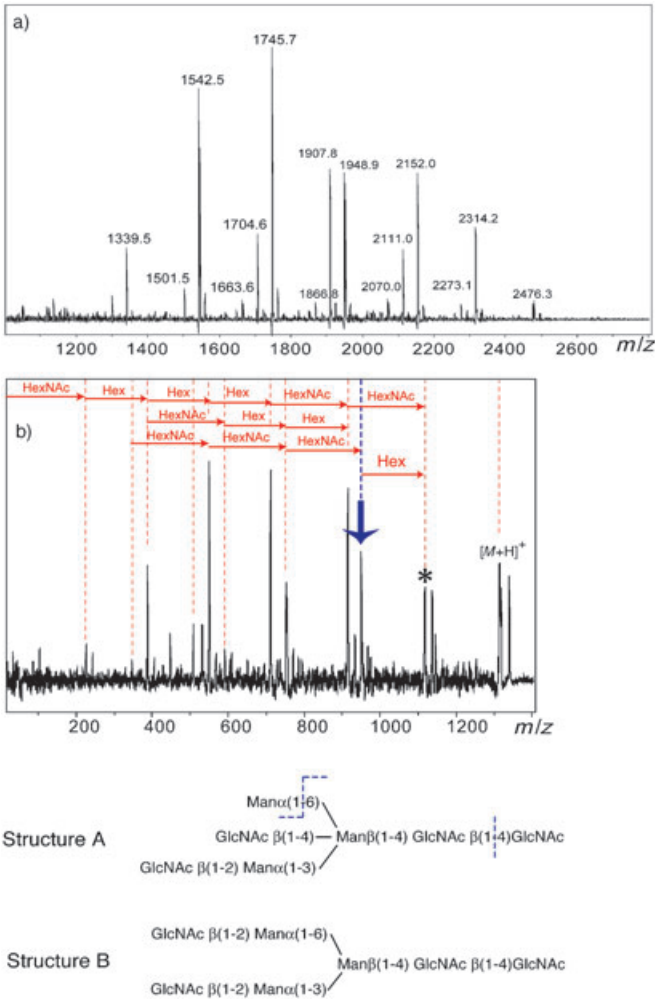

Figure 7. MALDI-TOF mass analysis of *N*-glycans released from ovalbumin. a) After isolation of *N*-glycans with the glycoblotting nanoparticles (**1/3**). b) LIFT TOF/TOF spectrum of signal (*m*/*z* 1339.5) in (a). The fragment ion indicated by asterisk corresponds to the loss of one GlcNAc from the reducing end, and the blue arrow indicates the fragment ion that consecutively loses one hexose from the nonreducing end.

Table 1. Hexose and HexNAc contents in possible oligosaccharide structures corresponding to signals in Figure 7a.

Observed *m*/*z*	$(Hex)_n(HexNAc)_m$		Calculated [*M*+Na]
	n	*m*	
1339.5	3	4	1339.48
1501.5	4	4	1501.53
1542.5	3	5	1542.56
1663.6	5	4	1663.59
1704.6	4	5	1704.61
1745.7	3	6	1745.63
1866.8	5	5	1866.67
1907.8	4	6	1907.69
1948.9	3	7	1948.72
2070.0	5	6	2069.75
2111.0	4	7	2111.77
2152.0	3	8	2151.80
2273.1	5	7	2272.82
2314.2	4	8	2313.85
2476.3	5	8	2475.90

oligosaccharide. For example, there are two possible *N*-glycan structures with *m*/*z* 1339.5 (structure **A** and **B** in Figure 7). From this TOF/TOF spectrum, the *m*/*z* 1339.5 peak can be identified as structure **A** because a fragment ion (y ion) that lacks one hexose unit from the nonreducing end was detected (blue arrow) indicating structure **A**. In the case of structure **B**, because both of the two nonreducing ends were GlcNAc residues, a fragment ion lacking only one hexose unit is not possible.

Comparison of glycopatterns between glycoblotting and a chromatographic method: For accurate and quantitative profiling of oligosaccharide (*N*-glycan) patterns, the glycoblotting nanoparticles should capture oligosaccharides independently of their structure. The proportion of oligosaccharides from crude samples purified by glycoblotting was compared to those purified by gel permeation chromatography (Biogel-P4). HPLC analysis combined with pyridylamine (PA) labeling[19] was carried out for oligosaccharides that were purified by glycoblotting or conventional gel permeation chromatography. Here, we used bovine asialofetuin, human IgG, and human serum as models for the study of *N*-glycan structures of single or mixed glycoproteins. Figure 8a and b show the HPLC analysis of *N*-glycans of bovine asialofetuin after purification by the two methods [a) for the glycoblotting and b) for chromatography]. Bovine asialofetuin has three main *N*-glycan components (I, II, and III, structures are shown in Figure 8c). The normalized relative intensity of all peaks are in good agreement between the two methods (Figure 8c). Similarly, human IgG *N*-glycans that contain core fucose were also elucidated and it was shown that the two purification methods produce an almost identical relative intensity for every oligosaccharide (Figure 8c). Finally, we used the glycoblotting method to isolate carbohydrates from human serum that contains a variety of glycoproteins. Because human serum contains a large amount of glucose that would inhibit the glycoblotting of released *N*-glycans, the glucose was transformed to glucolactone by a glucose oxidase prior to glycoblotting. The major *N*-glycans in the serum are a hybrid type with or without core fucose. We found that the relative molecular ratio after glycoblotting is identical to that after conventional chromatography. These results support the hypothesis that the nanoparticles trap all *N*-glycans with the same reaction efficiency, independent of the core fucosylation. Therefore, glycoblotting provides accurate ratios of the oligosaccharides in the sample.

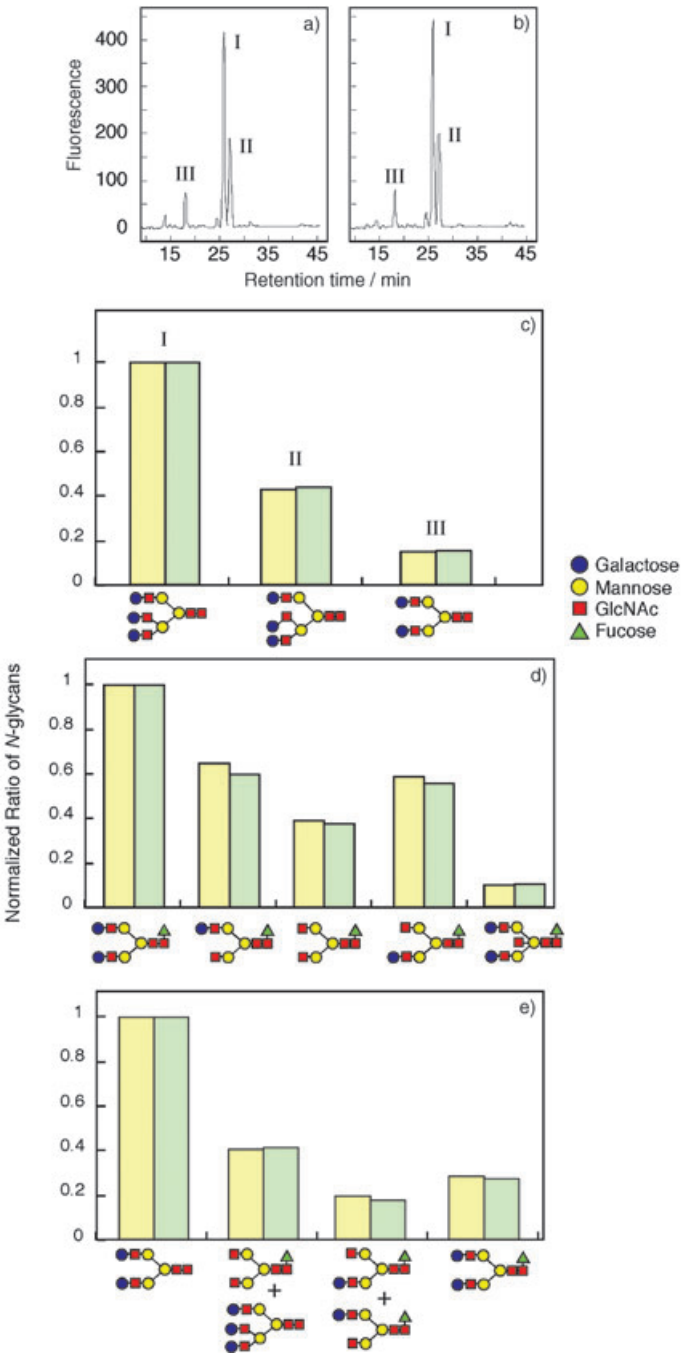

Figure 8. Comparison of *N*-glycans of glycoproteins purified by the glycoblotting process and by gel permeation chromatography. HPLC analysis of *N*-glycans of bovine asialofetuin purified by a) glycoblotting and b) gel permeation chromatography. The purified *N*-glycans was labeled with PA and analyzed by HPLC. The relative intensities of all peaks were normalized and are shown in bar graphs. c) Bovine asialofetuin. d) Human IgG. e) Human serum. Yellow bar: purification by glycoblotting, green bar: purification by gel permeation chromatography.

Glycoblotting of oligosaccharides contained in the skin of mice: To assess the feasibility of applying our approach to biological samples, we analyzed oligosaccharides in the skin of mice. Full-thickness skin samples were taken from the dorsal area of 7-week-old hairless mice. After peeling the epidermis from the dermis by heat separation, the dermis were washed with PBS and minced. Sialic acid residues were removed with HCl solution (pH 2.0) for 60 min at 90 °C. The crude sample was then treated with PNGase F to release the *N*-glycans. The oligosaccharides in this sample were extracted and purified with glycoblotting nanoparticles. The purified solution was analyzed by MALDI-TOF mass spectrometry (Figure 9). Each signal in the spectrum was identified using an oligosaccharide structure database (Gly-

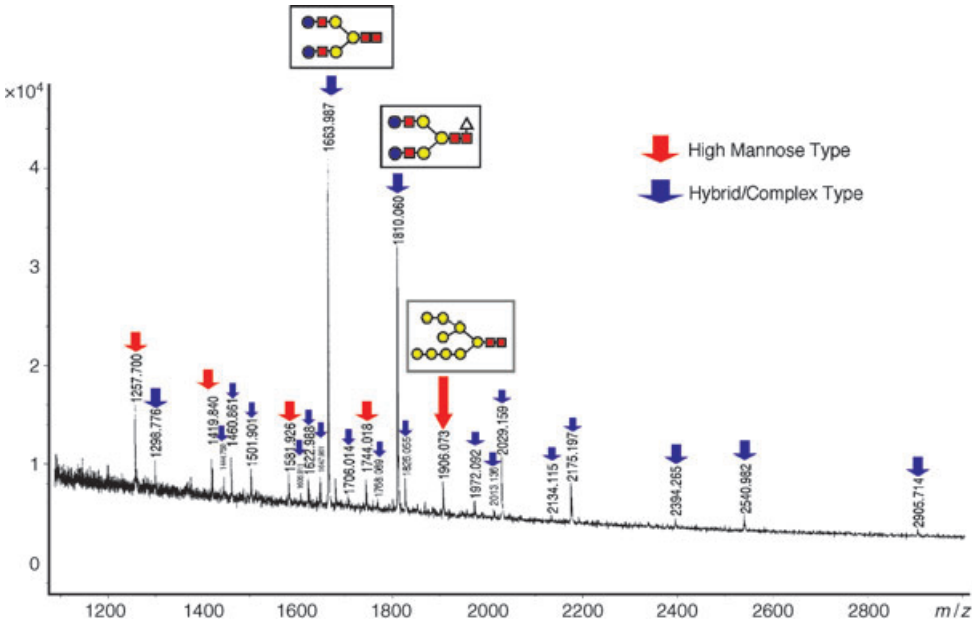

Figure 9. MALDI-TOF mass spectrum of *N*-glycans contained in mice dermis purified by glycoblotting. All peaks include a sodium cation.

coMod).[20] We found that the signals correspond to *N*-glycans of the complex/hybrid or the high mannose type. Three example structures were indicated in Figure 9. The oligosaccharides contained in mice dermis were also analyzed by conventional HPLC analysis combined with PA labeling. These data indicate that the major components are the two hybrid-type structures shown in Figure 9 (data not shown; however, a detailed analysis will be reported in near future). HPLC analyses also indicate that there were high mannose-type *N*-glycans ($Man_mGlcNAc_2$: m = 5–9) in the dermis of mice. Because the relative MALDI-TOF mass intensities of individual oligosaccharides are related to the distribution of oligosaccharides in the pool,[6,21] our glycoblotting procedure provides a rapid and quantitative method to reveal the glycosylation pattern in biological samples when combined with mass analysis.

Conclusion

This study demonstrates that glycoblotting based on a catch-and-release approach could be useful for specific capture of oligosaccharides. Our approach will greatly simplify the process of purification and isolation of small amounts of sugars from biological samples without any tedious techniques. Therefore, we believe that the combined use of glycoblotting and mass spectrometry provides a high-throughput glycoform analysis technique that will lead to early diagnoses and tailored treatment of a variety of diseases.

Experimental Section

General methods: 10,12-Pentacosadiynoic acid was purchased from Tokyo Kasei Co. (Japan). Boc-amino-oxyacetic acid was purchased from Novabiochem. All commercial reagents were used without further purification. Reactions were monitored by TLC on 250 μm silica gel plates (Merck, 60F254) by means of UV light and cerium molybdate solution (10% cerium(IV) sulfate, 15% H_2SO_4 aqueous solution). NMR spectra (500 MHz) were recorded on a Bruker AMX-500 instrument. All NMR measurements were carried out at room temperature in $CDCl_3$ or [D_4]methanol. MALDI-TOF MS were measured with an Ultraflex TOF/TOF mass spectrometer equipped with a reflector, and controlled by the Flexcontrol 1.2 software package (Brucker Daltonics GmbH, Bremen, Germany).

Pentacosa-10,12-diynoic acid {2-[2-(2-aminoethoxy)ethoxy]ethyl}amide (5): 1-Ethyl-3(3′-dimethylaminopropyl)carbodiimide-HCl (3.3 g, 17.2 mmol) was added to a mixture of 10,12-pentacosadiynoic acid (**4**, 1.6 g, 4.3 mmol) and 2,2′-(ethylenedioxy)bis(ethylamine) (5 mL, 34 mmol) in CH_2Cl_2 (300 mL) at 0 °C. The reaction mixture was stirred at 1) 0 °C for 1 h and 2) at room temperature for 8 h. The mixture was washed with water and brine, and then dried (Na_2SO_4). The solvent was evaporated in vacuo. The residue was purified by chromatography (silica gel, CH_2Cl_2/MeOH 7:3) to afford **5** as a white solid in 70% yield. ^{1}H NMR (500 MHz, $CDCl_3$): δ = 6.51 (s, 1H), 3.61 (m, 6H), 3.56 (t, 2H), 3.42 (t, 2H), 2.96 (t, 2H), 2.20 (m, 6H), 1.59 (m, 2H), 1.48 (m, 4H), 1.34 (m, 4H), 1.25 (m, 22H), 0.85 ppm (t, J = 6.90, 7.05 Hz, 3H); ESI MS (pos): m/z calcd for $C_{31}H_{57}N_2O_3$ $[M+H]^+$: 505.4; found: 505.4.

Diacetylene-functionalized *tert*-butoxycarbonyl-aminooxyl lipid (7): 1-Ethyl-3(3′-dimethylaminopropyl)carbodiimide-HCl (2.0 g, 10.4 mmol) was added to a solution of compound **5** (1 g, 1.98 mmol) and Boc-amino-oxyacetic acid (0.9 g, 4.7 mmol) in a mixed solvent (250 mL) of $CHCl_3$ and MeOH (95:5 v/v) at 0 °C. The reaction mixture was stirred for 12 h at room temperature. The mixture was washed with water and brine, and then dried (Na_2SO_4). The solvent was evaporated in vacuo. The residue was purified by chromatography (silica gel, CH_2Cl_2/MeOH 9:1 v/v) to afford **7** as a white solid in 94% yield. ^{1}H NMR (500 MHz, $CDCl_3$): δ = 7.96 (s, 1H), 6.18 (s, 1H), 4.35 (s, 2H), 3.66 (s, 4H), 3.60 (m, 4H), 3.54 (m, 2H), 3.47 (m, 2H), 2.26 (t, J = 6.93, 6.89 Hz, 4H), 2.20 (t, J = 7.46, 7.85 Hz, 2H), 1.77 (1H, s), 1.64 (2H, m), 1.53 (4H, m), 1.50 (9H, s), 1.39 (4H, m), 1.28 (22H, m), 0.90 ppm (t, J = 6.85, 7.09 Hz, 3H); ESI MS (pos): m/z calcd for $C_{38}H_{67}N_3O_7$ $[M+H]^+$: 678.5; found 678.4.

Diacetylene-containing aminooxyl lipid 1: Trifluoroacetic acid (10 mL) was added to a cold solution (0 °C) of compound **7** (0.5 g) in CH_2Cl_2 (50 mL). The reaction mixture was stirred at 0 °C for 5 h, and toluene (10 mL) was added. The solvents were evaporated in vacuo to afford pure compound **1** in a quantitative yield. ^{1}H NMR (500 MHz, $CDCl_3$): δ = 6.456 (s, 1H), 4.41 (s, 2H), 3.62–3.56 (m, 6H), 3.56–3.48 (m, 4H), 3.46–3.41 (m, 2H), 2.214 (t, J = 6.94 Hz, 4H), 1.6–1.2 (m, 36H), 0.857 ppm (t, J = 7.25 Hz, 3H); ^{13}C NMR (125 MHz, $CDCl_3$): δ = 175.69, 157.90, 114.44, 77.633, 77.441, 72.465, 70.046, 70.011, 69.825, 69.212, 65.313, 65.233, 39.526, 39.0312, 36.334, 31.917, 29.644, 29.624, 29.608, 29.478, 29.338, 29.134, 29.097, 29.076, 28.893, 28.873, 28.762, 28.375, 28.303, 25.744, 22.685, 19.199, 19.156, 14.100 ppm; ESI MS (pos): m/z calcd for $C_{33}H_{60}N_3O_5$ $[M+H]^+$: 578.45; found 578.42.

Methyl *tert*-butoxycarbonylaminooxyacetate (8): Boc-aminooxyacetic acid (1.50 g, 7.9 mmol) was dissolved in toluene/methanol (30 mL/

2.2 mL). TMS-diazomethane (2.0 M) in hexane (4.9 mL) was added, and the mixture was stirred for 1 h. The solvent was evaporated in vacuo, and the residue was subjected to column chromatography (silica gel, hexane/EtOAc 3:1) to give 1.5 g (93.4%) of **8**. ^{1}H NMR (500 MHz, $CDCl_3$): δ = 7.85 (s, 1H), 4.36 (s, 2H), 3.69 (s, 3H), 1.39 ppm (s, 9H).

Methyl (*tert*-butoxycarbonyl-*N*-methylaminooxy)acetate (9): Ester **8** (1.41 g, 6.86 mmol) was dissolved in DMF (150 mL). Sodium hydride (65%, 312 mg, 8.5 mmol) was added, and the mixture was stirred at room temperature. After 20 min, methyl iodide (510 μL) was injected to the reaction mixture and stirring was continued for 2 h at room temperature. The solvent was evaporated, and chloroform was added to the mixture. The solvent was washed with brine, dried over sodium sulfate, and evaporated. The residue was purified by column chromatography (silica gel, hexane/EtOAc 7:1) to give 1.22 g (81.3%) of **9**. ^{1}H NMR (500 MHz, $CDCl_3$): δ = 4.46 (s, 2H), 3.76 (s, 3H), 3.19 (s, 3H), 1.39 ppm (s, 9H).

(*tert*-Butoxycarbonyl-*N*-methylaminooxy)acetic acid (10): Ester **9** (95 mg, 0.46 mmol) was dissolved in methanol/H_2O (3 mL/1 mL) at 5°C. Sodium methoxide (89 μL of 28% w/w in methanol, 0.37 μmol) was added, and the mixture was stirred for 1 h. After neutralization with Amberlite resin, the resin was removed by filtration. The filtrate was concentrated to give **10** (90 mg, 95.4%). ^{1}H NMR (500 MHz, $CDCl_3$): δ = 4.45 (s, 2H), 3.20 (s, 3H), 1.50 ppm (s, 9H).

***tert*-Butoxycarbonyl-*N*-methylaminooxyl lipid (11)**: 1-Ethyl-3(3′-dimethylaminopropyl)carbodiimide–HCl (167 mg, 0.87 mmol), dimethylaminopyridine (1 mg, 8.2 μmol), and compound **5** (193 mg, 0.38 mmol) were added to a solution of compound **10** (90 mg, 4.39 mmol) in $CHCl_3$ (5 mL). The reaction mixture was stirred for 14 h at room temperature. The solvent was washed with brine, dried over sodium sulfate, and evaporated. The residue was purified by column chromatography (silica gel, $CHCl_3$/methanol 8:2) to give 87 mg (33%) of **11**. ^{1}H NMR (500 MHz, $CDCl_3$): δ = 8.23 (s, 1H), 6.23 (s, 1H), 4.31 (s, 2H), 3.62 (m, 4H), 3.59 (m, 2H), 3.54 (m, 2H), 3.50 (m, 2H), 3.45 (m, 2H), 3.11 (s, 3H), 2.23 (t, J = 6.98 and 6.97 Hz, 4H), 2.17 (t, J = 7.40 and 7.82 Hz, 2H), 1.61 (m, 2H), 1.51 (m, 4H), 1.49 (s, 9H), 1.35 (m, 4H), 1.28 (m, 22H), 0.87 ppm (t, J = 6.84 and 7.14 Hz, 3H); MALDI-TOF (pos) calcd for $C_{39}H_{70}N_3O_7$ $[M+H]^+$: 692.5; found 692.4.

Diacetylene-containing *N*-methylaminooxyl lipid 2: Trifluoroacetic acid (2 mL) was added to a cold solution (0°C) of compound **11** (87 mg) in CH_2Cl_2 (4 mL). The reaction mixture was stirred at 0°C for 10 min. Toluene (10 mL) was added, and the solvents were evaporated in vacuo to afford pure compound **2** in quantitative yield. ^{1}H NMR (500 MHz, $CDCl_3$): δ = 7.43 (s, 1H), 6.36 (s, 1H), 4.48 (s, 2H), 3.66 (s, 4H), 3.58 (m, 4H), 3.51 (m, 2H), 3.46 (m, 2H), 2.91 (s, 3H), 2.24 (t, J = 6.60 and 6.97 Hz, 4H), 2.20 (m, 2H), 1.60 (m, 2H), 1.52 (m, 4H), 1.37 (m, 4H), 1.28 (m, 22H), 0.90 ppm (t, J = 6.69 and 7.18 Hz, 3H); MALDI-TOF (pos) calcd for $C_{34}H_{62}N_3O_5$ $[M+H]^+$: 592.5; found 591.9.

Preparation of polymerized liposomes: Aminooxyl lipid **1** (1.5 mg, 1.58 mmol) and 1,2-bis(10,12-tricosadiynoyl)-*sn*-glycero-3-phosphocholine (**3**, 13.0 mg, 14.2 mmol) were dissolved in $CHCl_3$/MeOH (9/1) and the solvent was evaporated to yield a thin lipid film on the surface of the flask. Deionized water was added to the flask to adjust the concentration of the lipid to 0.3 mM. The aqueous solution was heated to 70°C and sonicated with a probe-type sonicator (Sonifier II, Branson Co.) for 10 min. The warm, clear solution containing the liposome was then cooled to 4°C and poured into a quartz cell. The solution was irradiated with a UV lamp (λ = 254 nm, 8 W, 100 Volt) under an argon atmosphere for 30 min. The distance of the lamp from the reaction cell was 10 cm.

SEM observation of photopolymerized liposomes: The morphological features of the fully photopolymerized liposomes (**1/3**) were examined under a Scanning Electron Microscope (SEM). The solution of liposomes in water was desiccated by vacuum drying, and the residue was coated with Pt/Pb (300 Å thickness) with an E-102 Hitachi Ion Sputter unit. SEM pictures were taken with an S-2250N Hitachi Scanning Electron Microscope, 15—25 kV/90–120 mA.

General procedure for glycoblotting (ovalbumin): Ovalbumin (1 mg) was heated at 90°C for 10 min in NH_4HCO_3 (10 mM) and lyophilized. The sample was treated with trypsin (50 μg) and chymotrypsin (50 μg) in Tris–HCl buffer (0.1 M, 0.2 mL, pH 8.0) at 37°C for 16 h. The reaction was terminated by heating to 90°C for 10 min. *N*-Glycosidase F (10 units, Roche Molecular Biochemicals) was added to the solution, and the mixture was stirred for 12 h at 37°C. The mixture was lyophilized to give a crude powder that was used as a sample for the glycoblotting. Glycoblotting nanoparticles (200 μL, 5 mg mL^{-1}) were added the crude solution (200 μL), and the pH was adjusted to 4.2 by adding sodium acetate buffer (1 M). The solution was incubated for 5 h at 40°C, then the nanoparticles were separated by means of a Microcon YM-50 centrifuge (10000 rpm) for 30 min at 24°C. The nanoparticles were washed with pure water (3×100 μL) in a centrifuge. Sulfonic acid–functionalized acidic resin (Amberlite IR-120) was suspended in the nanoparticle solution for 3 h at 37°C to release the trapped carbohydrates. The free carbohydrates were collected by centrifugation (10000 rpm for 30 min) in a Microcon YM-50. Prior to mass analysis, the carbohydrate solution was concentrated to 20 μL with a centrifugal evaporator at 50°C.

Preparation of matrix-sample crystals for MALDI-TOFMS: The matrix solutions were prepared as follows: α-cyano-4-hydroxycinnaminic acid (CHCA, Bruker Daltonics GmbH) was prepared as a saturated solution in acetonitrile/water (3:1 (v/v)). The matrix solution (0.5 μL) was applied to the target spot of an Anchorchip plate™ (Bruker Daltonics), which was equipped with 384 hydrophilic anchors on an otherwise hydrophobic surface, followed by application of the sample solution (1 μL). The plate was then dried at room temperature.

MALDI-TOF mass spectrometry: In the MALDI-TOFMS reflector mode, ions generated by a pulsed UV laser beam (nitrogen laser, λ = 337 nm, 5 Hz) were accelerated with 23.5 kV. Metastable ions generated by laser-induced decomposition of the selected precursor ions were analyzed without any additional collision gas.

In MALDI-TOF/TOF mode, precursor ions were accelerated to 8 kV and selected in a timed ion gate. The fragments were accelerated by 19 kV in the LIFT cell (LIFT means "lifting" of the potential energy for the second acceleration of the ion source), and their masses were analyzed after passage through the ion reflector. Masses were automatically annotated with the FlexAnalysis 2.0 software package. External calibration of MALDI mass spectra was carried out with reference to singly charged monoisotopic peaks of a mixture of human angiotensin II (m/z 1046.542), bombesin (m/z 1619.823), ACTH (18–39) (m/z 2465.199), and somatostatin 28 (m/z 3147.472). The mixture of these peptides was measured on a central spot of a 3×3 mm square by external calibration. To achieve a mass accuracy better than 60 ppm, internal calibration was carried out by doping the matrix solution with a mixture of the calibration peptides. Calibration of these mass spectra was performed automatically with a customized macro command of the FlexControl 2.1 software package. The macro command was used to calibrate the monoisotopic singly charged peaks of the above-mentioned peptides.

Preparation of mouse skin dermis: Male hairless mice (Hos/HR-1) were obtained from Nippon SLC (Shizuoka, Japan). Full-thickness skin samples were taken from the dorsal area of 7-week-old hairless mice. The epidermis was peeled from the dermis by heat separation (60°C, 30 s). The dermis were washed with PBS and minced, heated at 90°C for 10 min in water, defatted with chloroform/methanol, and then lyophilized. Sialic acid residues were removed with HCl (pH 2.0), for 60 min at 90°C. The crude carbohydrate mixtures were used for glycoblotting under the same conditions used for analyzing oligosaccharides from ovalbumin (pH 4.2, 5 h, 40°C).

Preparation and characterization of PA-oligosaccharides: To test the reliability of the glycoblotting method, released oligosaccharides were purified and converted to PA-oligosaccharides based on the conventional processes using Bio-Gel P-4 (1×38 cm) eluted with water. The purified oligosaccharides were lyophilized and pyridylaminated with 2-aminopyridine and sodium cyanoborohydride.[19] The PA-oligosaccharides were removed from any unreacted reagents with Sephadex G-15 (1×38 cm, eluted with 10 mM NH_4HCO_3). The purified PA-oligosaccharides were loaded onto an octadecylsilyl-silica column (ODS, 6×150 mm, Shimadzu, Kyoto, Japan) and subjected to HPLC (NANOSPACE SP-2 system, Shiseido, Tokyo, Japan) as follows: the solvent used for elution was sodium phosphate buffer containing 1-butanol (10 mM, pH 3.8), and the 1-butanol concentration was increased linearly from 0.1% to 0.25% (v/v) over a

period of 60 min. The flow rate was 1.0 mL per min and the column temperature was 55 °C. Elution time was variable, depending on the individual column, its age, or the batches of solvents. To reduce such errors, we revised the elution time to give a value in glucose units (GU). For each running batch, the PA-isomaltooligosaccharide (Seikagaku Co., Japan) mixture was analyzed. All elution times of the sample peaks were converted to a GU value, giving a number that indicates the degree of polymerization of the glucose residues.

Acknowledgements

This work was partly supported by a grant for the National Project on "Functional Glycoconjugate Research Aimed at Developing for New Industry" from the Ministry of Education, Science, and Culture of Japan and Tokuyama Science Foundation.

[1] R. Apweiler, H. Hermjakob, N. Sharon, *Biochim. Biophys. Acta* **1999**, *1473*, 4–8.
[2] R. B. Parekh, R. A. Dwek, D. J. Sutton, D. L. Fernandes, A. Leung, D. Stanworth, T. W. Rademacher, T. Mizuochi, T. Taniguchi, K. Matsuta, F. Takeuchi, Y. Nagano, T. Miyamoto, A. Kobata, *Nature* **1985**, *316*, 452–457.
[3] a) R. Kannagi, M. Izawa, T. Koike, K. Miyazaki, N. Kimura, *Cancer Sci.* **2004**, 95, 377–384; b) N. Sawabu, H. Watanabe, Y. Yamaguchi, K. Ohtsubo, Y. Motoo, *Pancreas* **2004**, *19*, 263–267; c) A. Varki, *Essentials of Glycobiology* (Eds.: A. Varki, R. Cummings, J. Esko, H. Freeze, G. Hart, J. Marth) Cold Spring Harbor Laboratory Press, New York, **1999**, pp.537–549.
[4] a) J. Hirabayashi, K. Hayama, H. Kaji, T. Isobe, K. Kasai, *J. Biochem.* **2002**, 132, 103–114; b) Z. Yang, W. S. Hancock, *J. Chromatogr.* **2004**, *1053*, 79–88; c) L. Xiong, D. Andrews, F. Regnier, *J. Proteome Res.* **2003**, 2, 618–625.
[5] Reinhold, Vernon. *PCT Int. Appl*. **2003** WO 03/08463 A1.
[6] S.-I. Nishimura, K. Niikura, M. Kurogochi, T. Matsushita, M. Fumoto, H. Hinou, R. Kamitani, H. Nakagawa, K. Deguchi, N. Miura, K. Monde, H. Kondo, *Angew. Chem.* **2004**, *117*, 93–98; *Angew. Chem. Int. Ed.* **2005**, *44*, 91–96.
[7] a) E. Fischer, *Ber. Dtsch. Chem. Ges.* **1884**, 17, 579; b) E. Fischer, *Ber. Dtsch. Chem. Ges.* **1887**, 20, 821.
[8] S. E. Cervigni, P. Dumy, M. Mutter, *Angew. Chem.* **1996**, *108*, 1325–1328; *Angew. Chem. Int. Ed. Engl.* **1996**, *35*, 1230–1232.
[9] a) B. Tieke, G. Wegner, D. Naegele, H. Ringsdorf, *Angew. Chem.* **1976**, *88*, 805–806; *Angew. Chem. Int. Ed. Engl.* **1976**, *15*, 764–765; b) T. Kuo, D. F. O'Brien, *Macromolecules* **1990**, *23*, 3225–3230.
[10] a) S. Okada, S. Peng, W. Spevak, D. H. Charych, *Acc. Chem. Res.* **1998**, *31*, 229–239; b) B. C. Roy, R. Peterson, S. Mallik, A. D. Campiglia, *J. Org. Chem.* **2000**, *65*, 3644–3651.
[11] K. Niikura, N. Osuga, N. Nagahori, R. Sadamoto, M. Shiono, N. Iwasaki, K. Monde, A. Minami, S.-I. Nishimura, *Polym. J.* **2004**, 36, 209–218.
[12] E. Kalb, S. Frey, L. K. Tamm, *Biochim. Biophys. Acta* **1992**, *1103*, 307–316.
[13] R. D. Marshall, *Annu. Rev. Biochem.* **1972**, *41*, 673–702.
[14] F. Peri, P. Dumy, M. Mutter, *Tetrahedron* **1998**, *54*, 12269–12278.
[15] a) Y. Iwasaki, A. Mikami, K. Kurita, N. Yui, K. Ishihara, N. Nakabayashi, *J. Biomed. Mater. Res.* **1997**, 36, 508–515; b) K. Ishihara, R. Aragaki, T. Ueda, A. Watenabe, N. Nakabayashi, *J. Biomed. Mater. Res.* **1990**, 24, 1069–1077; c) K. Ishihara, *Trends Polym. Sci.* **1997**, *5*, 401–407.
[16] a) D. J. Harvey, D. R. Wing, B. Kuster, I. B. Wilson, *J. Am. Soc. Mass Spectrom.* **2000**, *11*, 564–571; b) E. Lattova, H. Perreault, *J. Chromatogr.* **2003**, *1016*, 71–87; c) H. J. An, T. R. Peavy, J. L. Hendrick, C. B. Lebrilla, *Anal. Chem.* **2003**, *75*, 5628–5637.
[17] M. Kurogochi, T. Matsushita, S.-I. Nishimura, *Angew. Chem.* **2004**, *116*, 4163–4167; *Angew. Chem. Int. Ed.* **2004**, *43*, 4071–4075.
[18] M. Kurogochi, S.-I. Nishimura, *Anal. Chem.* **2004**, *76*, 6097–6101.
[19] H. Nakagawa, Y. Kawamura, K. Kato, I. Shimada, Y. Arata, N. Takahashi, *Anal. Biochem.* **1995**, 226, 130–138.
[20] http://kr.expasy.org/tools/glycomod/
[21] T. J. P. Naven, D. J. Harvey, *Rapid Commun. Mass Spectrom.* **1996**, *10*, 1361–1366.

Received: December 16, 2004
Published online: April 13, 2005